Springer

Journal of Mechanical Science and Technology 23 (2009) 3332~3339

Journal of Mechanical Science and Technology

www.springerlink.com/content/1738-494x
DOI 10.1007/s12206-009-1020-1

# Skew control of a quay container crane †

Quang Hieu Ngo[1] and Keum-Shik Hong[2,*]

[1]*School of Mechanical Engineering, Pusan National University, Busan 609-735, Korea*
[2]*Department of Cogno-Mechatronics Engineering and School of Mechanical Engineering, Pusan National University, Busan 609-735, Korea*

(Manuscript Received June 9, 2009; Revised Octorber 16, 2009; Accepted November 2, 2009)

**Abstract**

In this paper, the skew control of the load (container) in the quay crane used in the dockside of a container terminal is investigated. The mathematical model of the 3-dimensional (3D) motions of the load is first derived. The container hooked to a spreader is suspended by four ropes in air. When the container is accelerated by the trolley or is disturbed by winds, it will make a rotational motion (trim, list, and skew) as well as a sway motion in the vertical plane. In such a case, the position of the container becomes difficult to control accurately due to the rotational motion even with the sway motion under control. This paper proposes an input shaping technique for the skew control based on the 3D dynamics of the container. The adopted skew control system uses four electric motors to vary the length of the four ropes individually. Simulation results show the effectiveness of the proposed system in controlling the skew motion.

***Keywords*:** Container crane; Control system design; Input shaping control; Skew motion

## 1. Introduction

A gantry-type quay crane is widely used in the dockside of a container terminal to load/unload containers. The quay crane consists of three main parts: a gantry, a trolley(s), and a spreader. The gantry (structure) supports all equipment and can move along the dockside. The trolley moves perpendicular to the gantry motion along the boom in the upper part of the gantry and transfers containers from the ship to Automated Guided Vehicles (AGVs) or trucks and vice versa. The spreader grabs a container (there are various types of spreaders: twin twenty, tandem forty, etc.) while it is suspended typically by four flexible ropes from the trolley. By changing the lengths of the ropes, the container is hoisted up and down.

The load (container) grabbed by the spreader will have six degrees of freedom: three translational motions along the $X$, $Y$ and $Z$ axes and three rotational motions with respect to the three axes (trim, list, and skew motions), respectively, as shown in Fig. 1. In addition, there is a sway angle $\gamma$ between the lifting ropes and the vertical axis. The sway motion of the load occurs during the transportation of a load from one place to another when the load is subject to accelerations and decelerations. The sway is caused by the inertia of the load, and it is unavoidable, but its angle can be controlled by an experienced crane operator or a computerized controller.

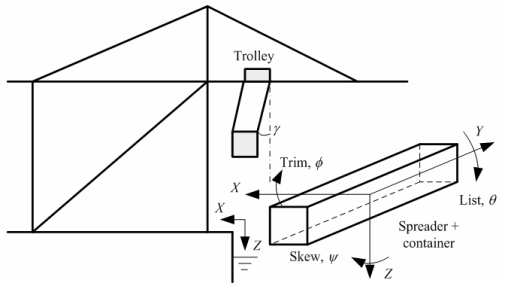


Fig. 1. Three rotational motions of the load (trim, list, and skew).

† This paper was recommended for publication in revised form by Associate Editor Kyung-Soo Kim

*Corresponding author. Tel.: +82 51 510 2454, Fax.: +82 51 514 0685
E-mail address: kshong@pusan.ac.kr

Many researchers have already investigated different types of sway controls. A modified input shaping control methodology had been presented to restrict the swing angle of the pay load within a specified value during the transfer to minimize the residual vibration at the end point [1]. Sorensen et al. [2] developed a combined feedback and input shaping controller enabling precise positioning and sway reduction in bridge and gantry cranes. Hong et al. [3] proposed a two-stage control of container cranes. The first stage control was a modified time-optimal control with feedback for the purpose of fast trolley traveling. The second stage control was a nonlinear control for the quick suppression of the residual sway while lowering the container at the target trolley position. The secondary control combined the partial feedback linearization to account for the unknown nonlinearities as much as possible and the variable structure control to account for the un-modeled dynamics and disturbances. Singhose et al. [4] proposed the command generation method of input shaping for reduction of the residual vibration. Terashima et al. [5] applied an optimal control method to suppress the sway of the load during transfer and the residual sway after transfer for a rotary crane in case the rope length was varied. Kim et al. [6] designed a state feedback controller with an integrator to control a real container crane. The inclinometer was used instead of a vision system, while providing almost the same performance. Park et al. [7] developed a nonlinear anti-sway controller crane with hoisting. A novel feedback linearization control law provided a simultaneous trolley position regulation, sway suppression and load hoisting control. Liu et al. [8] proposed a sliding mode fuzzy control for both X-direction and Y-direction transports. According to the influences on system dynamic performance, both the slope of sliding mode surface and the coordination between the two subsystems were automatically tuned by real time fuzzy inference respectively. Lee et al. [9] designed a sliding-mode anti-swing trajectory control scheme for overhead cranes based on the Lyapunov stability theorem, where a sliding surface, coupling the trolley motion with load swing, was adopted for a direct damping control of load swing. Vibration control methods were considering applying for container crane [10-12]. Variable structure control method is also a candidate for crane control [13].

On the other hand, the skew, list, and trim motions of the load are caused by the uneven distribution of the materials inside the container or misaligned ropes or other external disturbances like the wind. These unwanted motions sometimes greatly delay the positioning of the load on an AGV or a truck. Among these three rotational motions, the skew motion is known to be the most critical in an unmanned operation of a crane. It occurs if the lengths of the left and right ropes are not equal, causing a difference in the sway period between the left side and right side of the container. Skew motion can also be caused by side winds as well as an unbalanced distribution of goods in the container. Recently, an anti-skew device has been developed by Mitsubishi Heavy Industries Ltd. Company, Japan, but its performance is known to be limited [14].

Many researchers have focused on the position control of the load, assuming that the load is a particle moving in 3D space. Naturally, the load was assumed to be held by one rope [15-20]. However, the rigid body motion of a load cannot be discussed with a single rope formulation. In reality, once the skew motion occurs, the load itself as a rigid body may oscillate around the vertical axis, even though the center of mass of the load remains at the desired position. Thus, it takes a longer time in putting the container on a truck or an AGV. Hence, skew motion control is critical for the reduction of cycle time.

Two approaches for skew control are reported in the literature. The method in [21] directly applies (four) control forces to the spreader through the hoisting ropes to obtain the desired motion of the spreader (this approach will be pursued in this paper). The method in [22] shifts the pulleys in the left-hand side or right-hand side of the trolley, so that a skew torque from the trolley pulleys can be transmitted to the spreader. Specifically, the authors first described the 3D dynamic behavior of the container accounting for the sway and skew motions, and introduced a skew-drive-system consisting of a DC motor that can move one side (two ropes) of the hoist mechanism on the trolley forward and backward so that the ropes can apply a yaw torque to the spreader. Furthermore, a simple controller to stabilize the sway and skew motions of the container was also discussed. A fuzzy controller in [23] attempted the control of both the sway and skew motions of the spreader, simultaneously. The developed controller was shown to be effective in controlling the position of the container in the presence of winds and some uncertainties. However, the main drawback was the use of four auxiliary

ropes in addition to the existing main ropes.

In this paper, the dynamics of the load movement in 3D space, namely, three translational motions (*X*, *Y* and *Z*) and three rotational motions (trim, list, and skew), are first analyzed. Then, an input shaping controller with a position and velocity controller is designed. This controller uses four electric motors to control and stabilize the skew motion as well as vertical motion.

This paper is organized as follows. Section 2 describes the kinematic configuration of the trolley and spreader. Section 3 presents the control system design for skew motion control. Section 4 discusses the simulation results. Section 5 presents the conclusions.

## 2. Kinematics: trolley and spreader

To mathematically model the dynamics of the load, three coordinate frames are introduced. The first is a global reference coordinate frame attached to the crane main structure (if the global reference frame is affixed to the ground, a known transformation between the ground and the main structure has to be considered), the second is a local coordinate frame attached to the trolley (i.e., the trolley frame, in short, *T*-frame), and the last is another local coordinate frame attached to the geometric center of the spreader (i.e., the spreader frame, *S*-frame). Since the relationship between the global reference frame and the trolley frame can be predetermined from the motion plan of the trolley, only the relationship between the *T*-frame and the *S*-frame will be considered in this paper.

Fig. 2 depicts a configuration of the trolley and spreader. Let *O*-*XYZ* denote the *T*-frame; $T_i$, $i = 1,\ldots,4$, denote the locations of the four pulleys of the trolley and $p_{ti}$, $i = 1,\ldots,4$, denote the position vectors from the origin of the *T*-frame to $T_i$, where the subscript *t* denotes "trolley". Let *o*-*xyz* denote the *S*-frame; $S_i$, $i=1,\ldots,4$, denote the positions of four pulleys in the spreader, $p_{si}$, $i =1,\ldots,4$, denote the position vectors from the origin of the *S*-frame to $S_i$, where the subscript *s* denotes "spreader"; $u_i$, $i=1,\ldots,4$, denote the unit vectors from $S_i$ to $T_i$, respectively. Since all vectors can be written either in the *T*-frame or in the *S*-frame, a left-hand-side superscript *T* or *S* will be used to specifically identify the coordinate frame that is used: for example, ${}^{T}u_i$ denote the unit vectors in the *T*-frame. Moreover, the dimensions of the trolley and spreader are defined by $a_x \times a_y$ [m] and $b_x \times b_y$ [m], respectively.

Let $\phi$, $\theta$, and $\psi$ be the angles representing the roll (trim), pitch (list), and yaw (skew) motions of the spreader in the *T*-frame. Then, the coordinate transformation matrix from the *S*-frame to the *T*-frame, ${}^{T}R_S$, is defined as follows.

$$
\begin{aligned}
{}^{T}R_S &= R(z,\psi)R(y,\theta)R(x,\phi) \\
&= \begin{bmatrix}
\cos\psi\cos\theta & -\sin\psi\cos\phi+\cos\psi\sin\theta\sin\phi & \sin\psi\sin\phi+\cos\psi\sin\theta\cos\phi \\
\sin\psi\cos\theta & -\cos\psi\cos\phi+\sin\psi\sin\theta\sin\phi & -\cos\psi\sin\phi+\sin\psi\sin\theta\cos\phi \\
-\sin\theta & \cos\theta\sin\phi & \cos\theta\cos\phi
\end{bmatrix},
\end{aligned} \tag{1}
$$

where

$$
R(z,\psi)=\begin{bmatrix}\cos\psi & -\sin\psi & 0\\ \sin\psi & \cos\psi & 0\\ 0 & 0 & 1\end{bmatrix},
$$

$$
R(y,\theta)=\begin{bmatrix}\cos\theta & 0 & \sin\theta\\ 0 & 1 & 0\\ -\sin\theta & 0 & \cos\theta\end{bmatrix},
$$

$$
R(x,\phi)=\begin{bmatrix}1 & 0 & 0\\ 0 & \cos\phi & -\sin\phi\\ 0 & \sin\phi & \cos\phi\end{bmatrix}.
$$

The vectors representing the elongation of the ropes in the *T*-frame can be written as

$$
{}^{T}d_i = -{}^{T}p_{ti} + {}^{T}p + {}^{T}R_S\,{}^{S}p_{si}, \quad i=1,\ldots,4, \tag{2}
$$

where $d_i$ are the distance vectors from $T_i$ to $S_i$, and $p_{ti}$ are given as follows.

$$
\begin{aligned}
{}^{T}p_{t1} &= \begin{bmatrix}a_x/2\\ a_y/2\\ 0\end{bmatrix}, & {}^{T}p_{t2} &= \begin{bmatrix}-a_x/2\\ a_y/2\\ 0\end{bmatrix}, \\
{}^{T}p_{t3} &= \begin{bmatrix}-a_x/2\\ -a_y/2\\ 0\end{bmatrix}, & {}^{T}p_{t4} &= \begin{bmatrix}a_x/2\\ -a_y/2\\ 0\end{bmatrix}.
\end{aligned} \tag{3}
$$

$p$ is the distance vector from $O$ to $o$ as

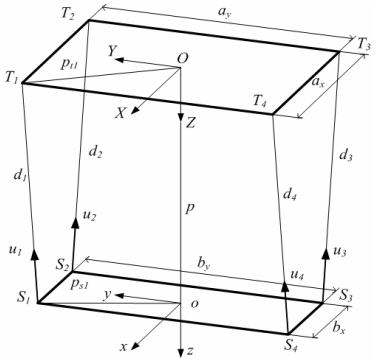


Fig. 2. Coordinates of the trolley, spreader, and cables.

$${}^{T}p = \begin{bmatrix} X & Y & Z \end{bmatrix}' \text{ (' denotes transpose).} \tag{4}$$

Similarly, $p_{si}$ are the position vectors from $o$ to $S_i$, given as follows.

$$\begin{aligned} {}^{S}p_{s1} &= \begin{bmatrix} b_x/2 \\ b_y/2 \\ 0 \end{bmatrix}, \quad {}^{S}p_{s2} = \begin{bmatrix} -b_x/2 \\ b_y/2 \\ 0 \end{bmatrix}, \\ {}^{S}p_{s3} &= \begin{bmatrix} -b_x/2 \\ -b_y/2 \\ 0 \end{bmatrix}, \quad {}^{S}p_{s4} = \begin{bmatrix} b_x/2 \\ -b_y/2 \\ 0 \end{bmatrix}. \end{aligned} \tag{5}$$

Therefore, the unit vectors along the rope in the $T$-frame can be expressed as

$${}^{T}u_i = -\frac{{}^{T}d_i}{\left\| {}^{T}d_i \right\|}, \quad i = 1,\ldots,4, \tag{6}$$

where $\|\cdot\|$ denotes the Euclidean norm. Hence, the forces along the ropes are given by

$${}^{T}F_i = {}^{T}u_i \left( k_s \varepsilon_i + k_d \dot{\varepsilon}_i \right), \quad i = 1,\ldots,4, \tag{7}$$

where $k_s$ is the stiffness, $k_d$ is the damping coefficient, and $\varepsilon_i$ is the stretch which depends on $L_i$ - the unloaded length of ropes $i$, computed as

$$\varepsilon_i = \left\| {}^{T}d_i \right\| - L_i, \tag{8}$$

where $L_i = L0_i + \Delta L_i$, $i = 1,\ldots,4$, $L_{0i}$ and $\Delta L_i$ are unloaded rope lengths and control inputs, respectively. Therefore, the resultant force acting on the spreader is the sum of four forces along the four ropes, ${}^{T}F_i$, together with the gravitational force $m{}^{T}g$. Thus, the acceleration vector at the center of gravity of the spreader becomes

$${}^{T}a = \frac{1}{m} \sum_{i=1}^{4} {}^{T}F_i + {}^{T}g. \tag{9}$$

Now, the velocity and displacement of the spreader at its mass center, ${}^{T}v$ and ${}^{T}p$, can be calculated by integrating (9).

On the other hand, the resultant moment acting on the spreader in the $T$-frame can be obtained as follows.

$${}^{T}M = \sum_{i=1}^{4} \left( {}^{T}p_{si} \times {}^{T}F_i \right), \tag{10}$$

where $\times$ denotes the cross-product operation. After transforming (10) into the $S$-frame, the rotational motion of the spreader in the $S$-frame can be expressed as follows [24, p. 166].

$$\left( {}^{T}R_S \right)^{-1} {}^{T}M = {}^{S}I \, {}^{S}\dot{\omega} + {}^{S}\omega \times ({}^{S}I \, {}^{S}\omega), \tag{11}$$

where ${}^{S}\omega = [\omega_x \quad \omega_y \quad \omega_z]'$ is the absolute angular velocity of the spreader, ${}^{S}\dot{\omega}$ is the rate of change of the angular velocity, and ${}^{S}I$ is the moment of inertia matrix, respectively, in the $S$-frame. Since the $S$-frame is affixed to the principle axes of the spreader, the moment of inertia matrix is given by

$${}^{S}I = \begin{bmatrix} I_x & 0 & 0 \\ 0 & I_y & 0 \\ 0 & 0 & I_z \end{bmatrix}. \tag{12}$$

Now, (11) can be rewritten as a differential equation as follows.

$${}^{S}\dot{\omega} = \left( {}^{S}I \right)^{-1} \left( \left( {}^{T}R_S \right)^{-1} {}^{T}M - {}^{S}\omega \times {}^{S}I \, {}^{S}\omega \right). \tag{13}$$

Note that the absolute angular velocity of the spreader in the $S$-frame, ${}^{S}\omega$, can be obtained by solving the differential Eq. (13).

Once the absolute angular velocity of the spreader in the $S$-frame is obtained, that in the $T$-frame (i.e., ${}^{T}\dot{\Theta} = [\dot{\phi} \quad \dot{\theta} \quad \dot{\psi}]'$) can be calculated as follows [24].

$${}^{S}\omega = \begin{bmatrix} \omega_x \\ \omega_y \\ \omega_z \end{bmatrix} = \begin{bmatrix} 1 & 0 & -\sin\theta \\ 0 & \cos\phi & \cos\theta\sin\phi \\ 0 & -\sin\phi & \cos\theta\cos\phi \end{bmatrix} \begin{bmatrix} \dot{\phi} \\ \dot{\theta} \\ \dot{\psi} \end{bmatrix} = J \, {}^{T}\dot{\Theta}, \tag{14}$$

where ${}^{T}\dot{\Theta} = [\dot{\phi} \quad \dot{\theta} \quad \dot{\psi}]'$ is the rates of change of the rotational angles of the spreader in the $T$-frame. Eq. (14) can be rewritten as

$${}^{T}\dot{\Theta} = J^{-1} \, {}^{S}\omega. \tag{15}$$

Now, the roll, pitch and yaw angles ($\phi$, $\theta$, and $\psi$) of the spreader can be found by integrating (15).

The state space formulation for the angular dynamics is given by

$$\begin{bmatrix} {}^{S}\dot{\omega} \\ {}^{T}\dot{\Theta} \end{bmatrix} = \begin{bmatrix} -\left({}^{S}I\right)^{-1} Q\, {}^{S}I & 0 \\ J^{-1} & 0 \end{bmatrix} \begin{bmatrix} {}^{S}\omega \\ {}^{T}\Theta \end{bmatrix} + \begin{bmatrix} \left({}^{S}I\right)^{-1} \left({}^{T}R_{S}\right)^{-1} \\ 0 \end{bmatrix} {}^{T}M \,, \tag{16}$$

where $Q = \begin{bmatrix} 0 & -\omega_z & \omega_y \\ \omega_z & 0 & -\omega_x \\ -\omega_y & \omega_x & 0 \end{bmatrix}$.

Finally, the above development on the dynamics of the spreader is summarized in Fig. 3.

## 3. Control system design

### *3.1 Control method*

In this paper, only the skew control is focused: The method of changing the lengths of four ropes is proposed. Four DC motors are controlled independently to vary the lengths of the ropes through ball screw-jacks. Each actuator extends or retracts at the desired amount so that the remaining length of the rope satisfies the kinematics constraint (2), and then the position and skew angle are defined, see Fig. 4. Determining the speed of the varying rope length is the main challenge for controlling the skew motion, because it affects directly the loading/unloading cycle times.

### *3.2 Position controller*

The skew system is configured with four DC motors, which are mechanically connected to ball screws. The end of each rope is connected directly to a ball nut. According to the motion of the DC motors, the ball nuts slide along the shaft of the ball screws. Through this movement, the lengths of the ropes are varied, the spreader motion is affected and the skew motion is performed. Without loss of generality, the DC motors can be modeled as a first-order system, and a conventional position controller of the DC motor can be used as shown in Fig. 6, where $k_p$ and $k_v$ are the position and velocity control gains, respectively, $k_a/(s+a)$ is the DC motor model and $k_{pitch}$ is a ratio constant depending on the screw pitch.

### *3.3 Input shaping technique*

Input shaping is a feed-forward control technique for improving the settling time and the positioning accuracy, while minimizing residual vibrations, of computer controlled machines. Input shaping is a strategy for the generation of time optimal shaped commands using only a simple model, which consists of the estimates of natural frequencies and damping ratios. Input shaping is implemented by convolving a desired system command signal with a sequence of impulses, so called input shaper, to produce a shaped input. The input shaper is chosen in such a way that in the absence of control input, it itself would not cause residual vibration. The result of the convolution is then used to drive the system. Some further study about input shaper design can be found in [25].

In this section, the Zero Vibration and Derivative (ZVD) shaper is designed to suppress the vibration of the spreader. The vibration can be reduced under a range of natural frequencies due to the robustness of the ZVD shaper. The parameters of the ZVD shaper (three impulses) are given by

Therefore, the control system is designed to control the rope length and the varying speed of the rope length as well as to suppress the skew oscillation. Two controllers are proposed to control the skew motion. The position controller is used to control the rope length and the varying speed of the rope length. The input shaping controller suppresses the residual vibration of the load. The skew control system diagram is shown in Fig. 5.

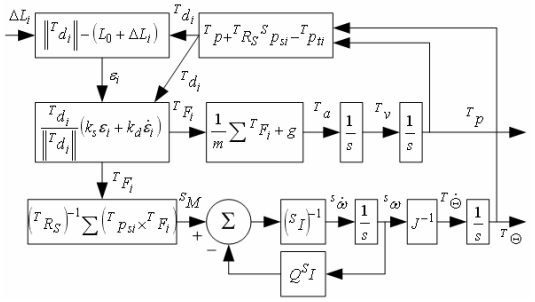


Fig. 3. Block diagram of the spreader dynamics.

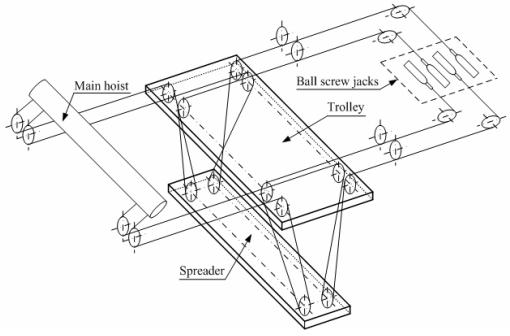


Fig. 4. Control scheme.

$$A_1 = \frac{1}{1+2K+K^2}, \quad t_1 = 0, \tag{17}$$

$$A_2 = \frac{2K}{1+2K+K^2}, \quad t_2 = \frac{\pi}{\omega_n\sqrt{1-\zeta^2}}, \tag{18}$$

$$A_3 = \frac{K^2}{1+2K+K^2}, \quad t_3 = 2t_2, \tag{19}$$

$$K = e^{\frac{-\zeta\pi}{\sqrt{1-\zeta^2}}}, \tag{20}$$

where $A_i$ is the amplitude of the $i$-th impulse and $t_i$ is the time of their application (time location - in seconds), $\omega_n$ is the natural frequency and $\zeta$ is the damping ratio of the residual vibration.

## 4. Measurement and simulation results

### *4.1 Natural frequency measurements*

To demonstrate the validity of the model, a test was performed at Gwangyang Container Terminal Port. A camcorder was used to record the vibration of the spreader during the test. Video files were analyzed to obtain the natural frequency of the spreader with and without a container at different heights (different rope lengths). The results are shown in Table 1.

### *4.2 Modeling*

Fig. 7 shows the modeling results – the natural frequency of the spreader – when the load was varied from 20 tons (empty) to 60 tons (full load) with the crane parameters in Table 2. By comparing the modeling and measurement results, it can be concluded that the mathematical model can describe exactly the dynamics of the spreader (the error is less than 6%).

### *4.3 Controlling*

The input shaping controller was used to suppress the residual skew vibration of the load. However, the fixed parameters of the input shaping controller were not suitable due to the varying of the rope lengths and the container mass. Hence, the parameters of the input shaping controller are predetermined. The amplitudes of the impulses of the ZVD shaper can be fixed parameters, [*A*1 *A*2 *A*3] = [0.25 0.5 0.25]. Because the rope lengths and the container mass varied, the locations of the impulses of the ZVD shaper varied with time, as shown in Table 3. When the controller was implemented, the control parameters are obtained from the table.

Table 1. Natural frequency of the spreader (with and without container) at certain length (Gwangyang Container Terminal Port), wind speed: 10 m/s.

| Load | Rope length [m] | Natural frequency [rad/s] |
|---|---|---|
| Spreader 40 ft (20 tons) | 36.561 | 0.583 |
| | 31.561 | 0.664 |
| | 26.561 | 0.751 |
| Container and Spreader 40 ft (25 tons) | 36.561 | 0.531 |
| | 31.561 | 0.586 |
| | 26.561 | 0.702 |

Table 2. System characteristics.

| | |
|---|---|
| Trolley ($a_x \times a_y$) [m] | 5.4×2.3 |
| Spreader ($b_x \times b_y$) [m] | 5.4×1.0 |
| Cable diameter [mm] | 30 |
| Container type | 40 ft |

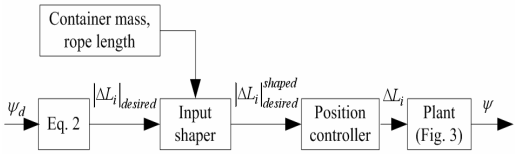


Fig. 5. Skew control diagram.

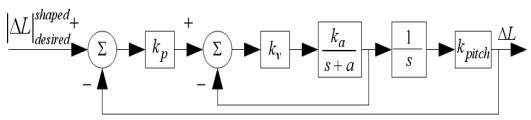


Fig. 6. Position control diagram.

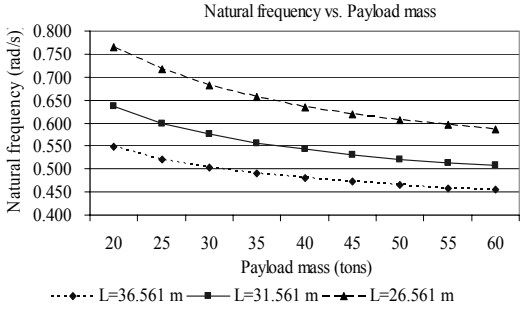


Fig. 7. Natural frequency of skew motion with different masses and rope lengths.

Table 3. Input shaper parameters.

| Rope length [m] | Mass [tons] | Designed natural frequency [rad/s] | $t_2$ [s] |
|---|---|---|---|
| 20 – 25 | 20 – 30 | 0.888 | 3.54 |
| | 30 – 40 | 0.795 | 3.95 |
| | 40 – 50 | 0.740 | 4.24 |
| 25 – 30 | 20 – 30 | 0.705 | 4.45 |
| | 30 – 40 | 0.643 | 4.88 |
| | 40 – 50 | 0.607 | 5.18 |
| 30 – 35 | 20 – 30 | 0.592 | 5.30 |
| | 30 – 40 | 0.548 | 5.73 |
| | 40 – 50 | 0.523 | 6.01 |
| 35 – 40 | 20 – 30 | 0.517 | 6.08 |
| | 30 – 40 | 0.484 | 6.49 |
| | 40 – 50 | 0.465 | 6.75 |

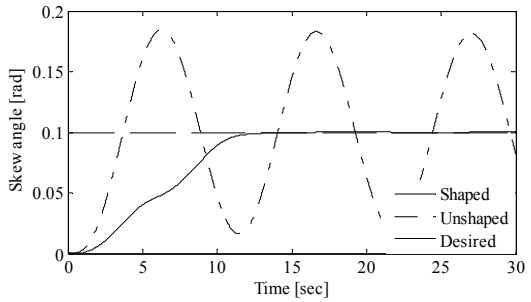


Fig. 8. System response – skew control.

Fig. 8 presents the response of the skew motion when the rope length was 27 m and the mass of payload was 42 tons (including container and spreader masses). When the spreader moved to the target position, the skew vibration converged to zero with the application of the input shaping controller.

## 5. Conclusions

A new type of skew motion control system was developed and applied to a container crane. Skew motion control was satisfied by the system verification test. We are planning to further improve the performance and function of the skew control system by accumulating performance records of its application to real cargo work operation. Furthermore, the exact parameters of the container crane should be calculated to define the controller parameters and thus, to improve the performance of the skew controller.

## Acknowledgment

This work was supported by the Mobile Harbor Project of the Korea Advanced Institute of Science and Technology funded by the Ministry of Education, Science, and Technology, Korea.

## References

[1] K. T. Hong, C. D. Huh and K. S. Hong, Command shaping control for limiting the transient sway angle of crane systems, *International Journal of Control, Automation and System* 1 (1) (2003) 43-53.

[2] K. L Sorensen, W. Singhose and S. Dickerson, A controller enabling precise positioning and sway reduction in bridge and gantry cranes, *Control Engineering Practice* 15 (7) (2007) 825-837.

[3] K. S. Hong, B. J. Park and M. H. Lee, Two-stage control for container cranes, *JSME International Journal, Series C* 43 (2) (2000) 273-282.

[4] W. Singhose, L. Perter, M. Kenison and E. Krrikku, Effects of hoisting on the input shaping control of gantry cranes, *Control Engineering Practice* 8 (10) (2000) 1159-1165.

[5] K. Terashima, Y. Shen and K. Yano, Modeling and optimal control of a rotary crane using the straight transfer transformation method, *Control Engineering Practice* 15 (9) (2007) 1179-1192.

[6] Y. S. Kim, K. S. Hong and S. K. Sul, Anti-sway control of container cranes: Inclinometer, observer, and state feedback, *International Journal of Control, Automation, and Systems* 2 (4) (2004) 435-449.

[7] H. Park, D. Chwa and K. S. Hong, A feedback linearization control of container cranes: Varying rope length, *International Journal of Control, Automation, and Systems* 5 (4) (2007) 379-387.

[8] D. Liu, J. Yi, D. Zhao and W. Wang, Adaptive sliding mode fuzzy control for a two-dimensional overhead crane, *Mechatronics* 15 (5) (2005) 505-512.

[9] H. H. Lee, Y. Liang and D. Segura, A sliding-mode anti-swing trajectory control for overhead cranes with high-speed load hoisting, *ASME Journal of Dynamic Systems, Measurement, and Control* 128 (4) (2006) 842-845.

[10] J. H. Park and S. Rhim, Experiments of optimal delay extraction algorithm using adaptive time-delay filter for improved vibration suppression, *Journal of Mechanical Science and Technology* 23 (4) (2009) 997-1000.

[11] A. Turnip, K. S. Hong and S. Park, Modeling of a hydraulic engine mount for active pneumatic engine

vibration control using the extended Kalman filter, *Journal of Mechanical Science and Technology* 23 (1) (2009) 229-236.

[12] S. H. Cho and S. Helduser, Robust motion control of a clamp-cylinder for energy-saving injection moulding machines, *Journal of Mechanical Science and Technology* 22 (12) (2008) 2445-2453.

[13] C. G. Kang, Variable structure fuzzy control using three input variables for reducing motion tracking errors, *Journal of Mechanical Science and Technology* 23 (5) (2009) 1354-1364.

[14] Mitsubishi Heavy Industries, Ltd., (2008). http://www.mhi.co.jp/en/products/detail/technology.html

[15] B. d'Andréa-Novel and J. M. Coron, Exponential stabilization of an overhead crane with flexible cable via a back-stepping approach, *Automatica* 36 (4) (2000) 587-593.

[16] H. Kawai, Y. B. Kim and Y. W. Choi, Anti-sway system with image sensor for container cranes, *Journal of Mechanical Science and Technology* 23 (10) (2009) 2757-2765.

[17] H. C. Cho, J. W. Lee, Y. J. Lee and K. S. Lee, Lyapunov theory based robust control of complicated nonlinear mechanical systems with uncertainty, *Journal of Mechanical Science and Technology* 22 (11) (2008) 2142-2150.

[18] H. C. Cho and K. S. Lee, Adaptive control and stability analysis of nonlinear crane systems with perturbation, *Journal of Mechanical Science and Technology* 22 (6) (2008) 1091-1098.

[19] C. W. Kim, K. S. Hong and H. Park, Boundary control of an axially moving string: actuator dynamics included, *Journal of Mechanical Science and Technology* 19 (2005) 40-50.

[20] M. I. Solihin and Wahyudi, Sensorless anti-swing control for automatic gantry crane system: Model-based approach, *International Journal of Applied Engineering Research* 2 (1) (2007) 147-161.

[21] B. Henriksson, (Applicant ABB AB), Load control device for a crane, European Patent (2008) (No. EP 1 894 881 A2).

[22] J. B. Klaassens, G. Honderd, A. E. Azzouzi, K. C. Cheok and G. E. Smid, 3D modeling visualization for studying controls of the Jumbo container crane, *Proceedings of the American Control Conference*, California, USA, (1999) 1754-1758.

[23] J. W. Lee, D. H. Kim and K. T. Park, Fuzzy control of sway and skew of a spreader by using four auxiliary cables, *Proceedings of International Conference on Control, Automation, and Systems*, Gyeonggi-Do, Korea, (2005) 1723-1728.

[24] D. T. Greenwood, *Advanced Dynamics*, Cambridge University Press, New York, USA, (2003).

[25] T. Singh and W. Singhose, Tutorial on input shaping/time delay control of maneuvering flexible structures, *Proceedings of the American Control Conference*, Anchorage, USA. (2002) 1717-1731.

**Quang Hieu Ngo** received the B.S. degree in mechanical engineering from Ho Chi Minh City University of Technology, Vietnam, in 2002, the M.S. degree in mechatronics from Asian Institute of Technology, Thailand, in 2007. He is currently a Ph.D. candidate in the School of Mechanical Engineering, Pusan National University, Korea. His research interests include port automation, control of axially moving systems, adaptive control, and input shaping control.

**Keum-Shik Hong** received the B.S. degree in mechanical design and production engineering from Seoul National University in 1979, the M.S. degree in ME from Columbia University in 1987, and both the M.S. degree in applied mathematics and the Ph.D. degree in ME from the University of Illinois at Urbana-Champaign in 1991. Dr. Hong serves as Editor-in-Chief of the Journal of Mechanical Science and Technology. He served as an Associate Editor for Automatica (2000-2006) and as an Editor for the International Journal of Control, Automation, and Systems (2003-2005). Dr. Hong received Fumio Harashima Mechatronics Award in 2003 and the Korean Government Presidential Award in 2007. His research interests include nonlinear systems theory, adaptive control, distributed parameter system control, robotics, and vehicle controls.